J. Fluid Mech. (1970), *vol.* 44, *part* 4, *pp.* 721–740
Printed in Great Britain

The formation of streamwise vorticity in turbulent flow

By H. J. PERKINS†
Engineering Department, Cambridge University

(Received 8 September 1969 and in revised form 9 April 1970)

Mean streamwise vorticity in turbulent flow is shown to arise both from mean flow skewing and from the inhomogeneity of anisotropic wall turbulence. The structure of the Reynolds stress tensor is examined in several flows where the latter mechanism predominates. On the basis of a simple model for the anisotropy, the direction of the secondary currents is deduced for the corner boundary layer, the salient edge flow, and in the non-uniform nominally two-dimensional boundary layer.

1. Introduction

Steady secondary currents in fluid flow have been formally separated into two categories by Prandtl (1952). Secondary flows of the first kind, derived from mean flow skewing, are in general qualitatively well understood, whilst those of the second kind, caused by non-uniformities in wall turbulence, are as yet not fully explained. This paper is concerned with flows falling in the latter category.

Historically, the analysis of secondary flows has proved most fruitful when attention is concentrated on the component of vorticity in the chosen primary direction. In steady incompressible constant-property flow, the mean streamwise‡ vorticity equation is

$$U\frac{\partial\xi}{\partial x}+V\frac{\partial\xi}{\partial y}+W\frac{\partial\xi}{\partial z}=\nu\nabla^2\xi+\xi\frac{\partial U}{\partial x}+\eta\frac{\partial U}{\partial y}+\zeta\frac{\partial U}{\partial z}+\underbrace{\frac{\partial}{\partial x}\left(\frac{\partial\overline{uv}}{\partial z}-\frac{\partial\overline{uw}}{\partial y}\right)}_{P_2}$$
$$\underbrace{\qquad\qquad}_{P_1}$$
$$+\underbrace{\frac{\partial^2}{\partial y\,\partial z}(\overline{v^2}-\overline{w^2})}_{P_3}+\underbrace{\left(\frac{\partial^2}{\partial z^2}-\frac{\partial^2}{\partial y^2}\right)\overline{vw}}_{P_4},\quad(1)$$

in which
$$\xi=\partial W/\partial y-\partial V/\partial z,$$
$$\eta=\partial U/\partial z-\partial W/\partial x,$$
and
$$\zeta=\partial V/\partial x-\partial U/\partial y,$$

using the notation of figure 1. This equation is most readily derived by eliminating the pressure, p, between the time-averaged Reynolds equations in the y and z directions.

† Present address: G.E.C. Power Engineering Ltd, Whetstone, Leicester.

‡ 'Streamwise' will be used to refer to the primary direction, x, which will also be the direction of the undisturbed free stream.

Terms on the left-hand side represent the convection of streamwise vorticity by the primary and secondary flows, or the total convection, $U_s \partial\xi/\partial s$, where s is the co-ordinate along the local streamline. On the right-hand side, the first term accounts for the viscous diffusion of streamwise vorticity and the second represents streamwise vortex stretching. Taken together, the next two terms,

$$P_1 = \eta \frac{\partial U}{\partial y} + \zeta \frac{\partial U}{\partial z} = \frac{\partial U}{\partial z}\frac{\partial V}{\partial x} - \frac{\partial U}{\partial y}\frac{\partial W}{\partial x} \tag{2}$$

describe the production of streamwise vorticity through the deflexion, or skewing, of the mean shear by a transverse pressure gradient or body force.

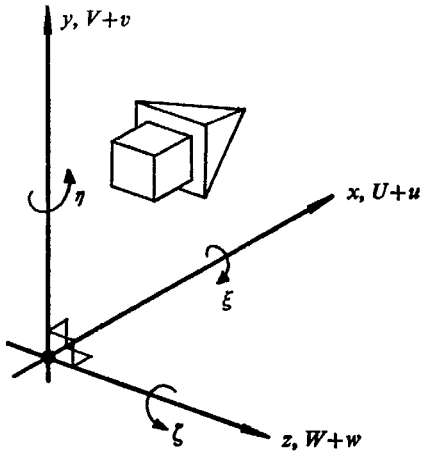

FIGURE 1. The co-ordinate system.

Secondary flows generated by this mechanism are of Prandtl's first kind and have received considerable attention since the early inviscid analyses of Squire & Winter (1951) and Hawthorne (1951). The usefulness of the latter in explaining flow behaviour in the outer region of a skewed turbulent boundary layer has been pointed out by many authors, notably Taylor (1959).

The remaining three terms of equation (1), present only in the turbulent layer, are responsible for maintaining secondary currents of Prandtl's second kind. Collectively these terms represent the sum effect of the time-averaged convection of turbulent vorticity by the turbulence plus the time-averaged production of turbulent vorticity; the latter by interactions identical to those of equation (2), but on an unsteady macro-scale. Prandtl first postulated the existence of such secondary currents to explain the isovel (line of constant velocity) distortions he observed in the duct flow measurements of Nikuradse & Schiller, as early as 1926. In straight non-circular ducts or channels he envisaged a system of longitudinal spirals in the flow conveying momentum into the corner regions. This required that velocity fluctuations tangential to the isovel exceed those perpendicular to the isovel so that a centrifugal acceleration is induced in regions of isovel curvature, propelling fluid radially outwards. Secondary currents, he concluded, must therefore be established in the direction of the isovel distortions and be supported by the anistropy of the turbulent direct stresses. All sub-

sequent secondary flow measurements in fully-developed (axially-homogeneous) straight non-circular duct flows have substantiated this qualitative argument. Attempts at a more rigorous explanation, notably by Einstein & Li (1958) and Hinze (1967), have shown that secondary currents of the second kind are produced by the non-uniformities in anisotropic wall turbulence. Figure 2, for example, demonstrates how the term P_3 is able to produce a rotational acceleration of a fluid element about the streamwise axis.

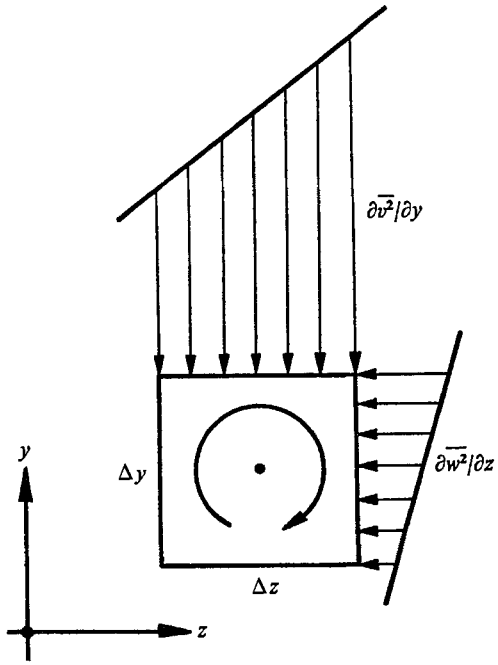

FIGURE 2. Mechanism of vorticity production by the direct stresses. $[\partial/\partial z\,(\partial\overline{v^2}/\partial y) - \partial/\partial y\,(\partial\overline{w^2}/\partial z)] > 0$ inducing a clockwise rotation, $\xi > 0$.

Clearly, anisotropic wall turbulence in any boundary-layer situation is potentially a source of the latter secondary currents whenever the flow is additionally inhomogeneous parallel to the bounding surfaces in the y, z plane. This occurs principally in the non-circular duct or in boundary regions formed at the streamwise corner or edge of a surface. The resulting secondary currents are invariably of a weak streamwise cellular vortex form, the helix angle being typically less than three degrees in the constant-pressure layer.

The form of the Reynolds stress tensor† in such flows is examined with particular reference to the terms of (1), which is shown to undergo considerable simplification in fully-developed or slowly-developing flows. Empirical observations in the zero-pressure-gradient turbulent corner boundary layer are extended to deduce the *direction* of the secondary currents in other flow situations where this simplified form of the streamwise vorticity equation might be expected to

† Throughout this paper the double velocity correlations at a point in the flow will be referred to as Reynolds stresses. The omission of the density multiplier in incompressible flow is merely a convenience.

apply. Three examples in which secondary currents of the second kind are known to arise will be discussed: (i) a nominally two-dimensional boundary layer with transverse non-uniformities; (ii) the flow along a salient edge; and (iii) the flow along the right-angled intersection of two plane surfaces.

2. The Reynolds stress tensor in transverse inhomogeneous flow

The earliest recorded measurements of the nine dependent variables, that is, U, V, W, and the six non-zero components of the Reynolds stress tensor, are those of Brundrett (1963) (Brundrett & Baines 1964) for fully-developed turbulent flow along a straight square duct. Stress measurements are also presented for ducts of rectangular and elliptic cross-section (aspect ratios of 3 and 2 respectively), relative to a Cartesian co-ordinate system having x along the duct axis and y and z parallel to the walls of the former, and aligned to the major and minor axes of the latter. The hot-wire procedure involved rotating a single inclined sensor to eight different orientations at each point in the flow, so that the stress $\overline{vw}$ and the difference $(\overline{v^2}-\overline{w^2})$ emerge as functions of four measured r.m.s. voltages. Perkins (1969) has shown that the accuracy of this method is very poor, a reading error of as little as $\pm 1\,\%$ in each r.m.s. voltage inducing, in $\overline{vw}$, an error of $\pm 100\,\%$ in the square duct, for example. However, it was shown that $\overline{vw}$, in the elliptic conduit, has a magnitude comparable with the wall shear stress over much of the flow, unlike the square or rectangular duct, where its value is approximately zero except in the immediate neighbourhood of the corner angle bisector plane. Their attempt to compute terms P_3 and P_4 of (1) must be regarded as inconclusive in view of the considerable scatter inherent in the stress measurements. The results of Gessner (1964*a*), (Gessner & Jones 1965) largely substantiate the findings of Brundrett although ducts of larger cross-section were used together with improved measuring techniques. The use of an X array hot-wire probe in conjunction with an adding/subtracting circuit (Gessner 1964*b*) gave considerably greater accuracy for $\overline{vw}$ and $(\overline{v^2}-\overline{w^2})$. The directional properties of the secondary correlation were also examined along an isovel, measuring in a 'floating' co-ordinate system (x, α, β), to locate planes in which $\overline{v_\alpha v_\beta}$ was zero. Such planes were not found to lie perpendicular to the isovels although earlier measurements (Gessner & Jones 1961) indicated that the ratio $\overline{v_\alpha^2}/\overline{v_\beta^2}$ takes its maximum value and is greater than unity when the (α, β) co-ordinates are located roughly tangential and normal to the local isovel.

The author has recently completed what is believed to be the first detailed survey of the mean and turbulent characteristics of a symmetrical boundary layer developing at approximately constant pressure (and also in diffusing flow), along the right-angled corner of a square-sectioned duct. The research programme is described fully in Perkins (1970) and relevant portions are summarized here in an appendix. With a view to computing the terms of (1), special attention has been paid to establishing an accurate hot-wire procedure, details of which are given in Perkins (1969). The representative boundary-layer cross-section used as an example in the present paper is situated 51·75 inches downstream of a trip wire in the constant-pressure layer, the mean velocity field being as illustrated in figure 3. The individual Reynolds stress components, omitted here for brevity,

behave almost exactly as in the fully-developed square duct flow of Gessner, although of a marginally lower magnitude, in general, and becoming asymptotically small or zero in the free stream. The symmetry of the stress field is excellent and satisfactorily reflected in figure 3.

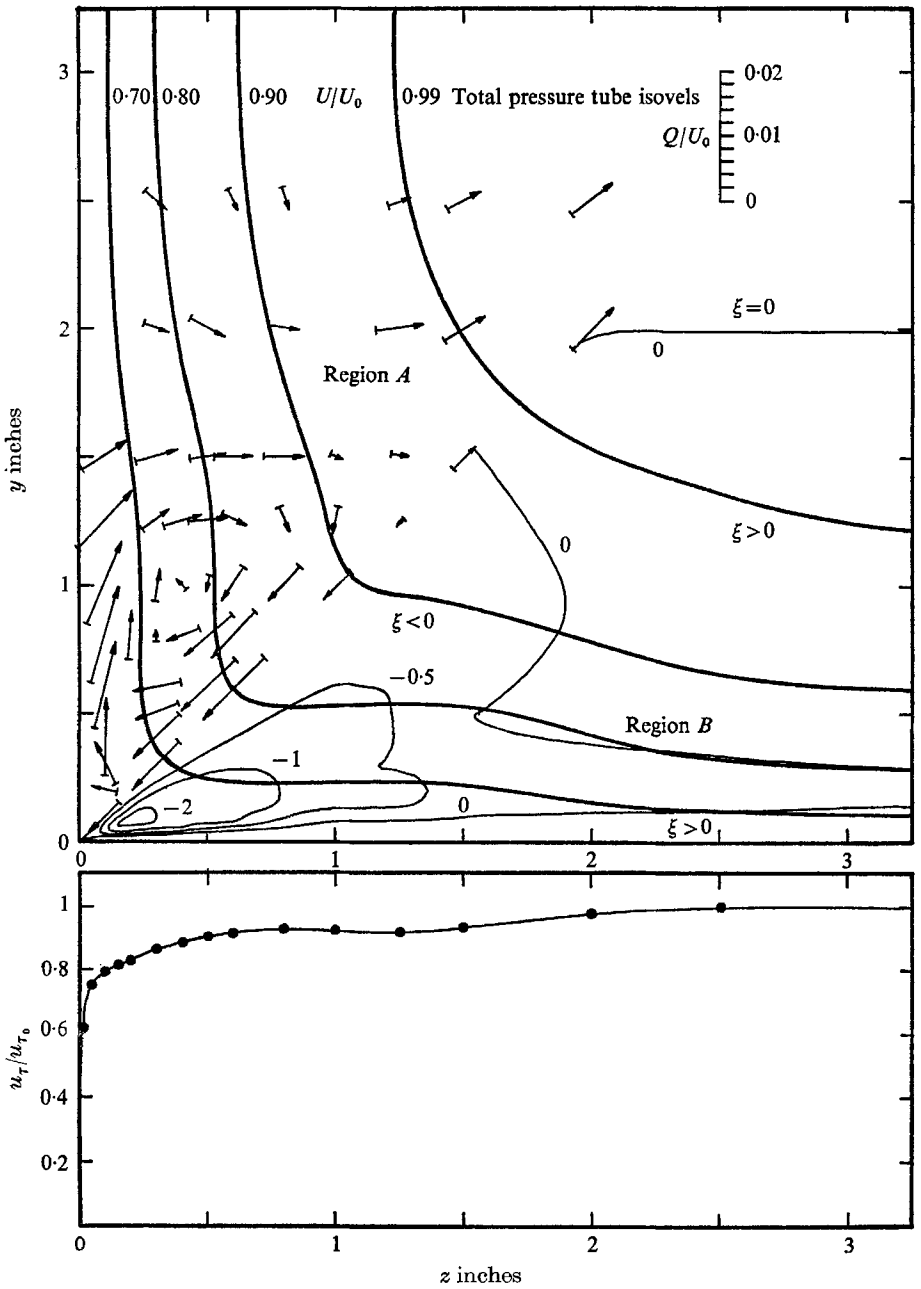

FIGURE 3. The corner boundary layer, ($U_0 = 56{\cdot}70$ ft./sec, $\partial p/\partial x \approx 0$). Region A: secondary flow vectors $Q = (V^2 + W^2)^{\frac{1}{2}}$. Region B: non-dimensional vorticity contours, $10\xi a/U_0$, $a = 1{\cdot}30$ inches. Wall shear velocity distribution on the $y = 0$ surface.

Having established the source of the data it is now possible to proceed with the examination of the stress tensor.

(*a*) *The primary shear stresses,* $\overline{uv}$ *and* $\overline{uw}$

The orientation of the resultant primary shear stress $\overline{uv_\beta} = (\overline{uv}^2 + \overline{uw}^2)^{\frac{1}{2}}$ is shown in figure 4 (region A) for fully-developed square duct flow, in figure 5 for a super-elliptic duct having a wall shape described by $y^4 + z^4 =$ constant, and in figure 6

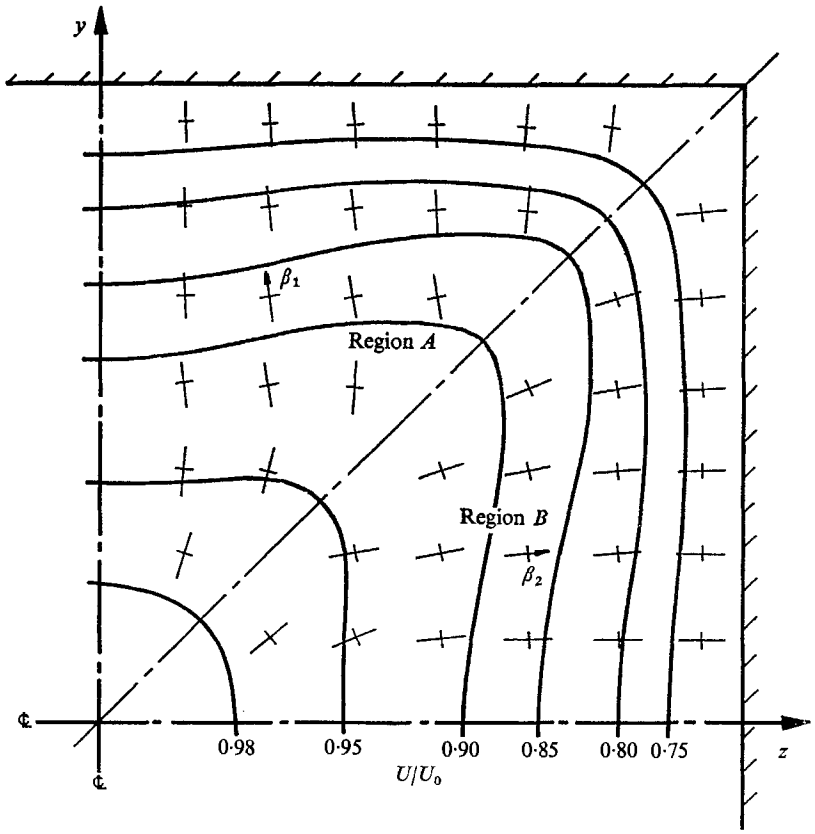

FIGURE 4. Square duct flow, Re† = 83,000 (after Brundrett 1963). Region A: direction of resultant shear stress, $\overline{uv_\beta} = (\overline{uv}^2 + \overline{uw}^2)^{\frac{1}{2}}$. Region B: orientation of planes in which $(\overline{v_\alpha v_\beta})_2 = 0$.

† Based on mean through-flow velocity and hydraulic diameter.

(region B) for the corner boundary layer. In each case the β_1 co-ordinate, aligned to the resultant primary shear stress, is seen to lie approximately perpendicular to the isovels, that is, in the direction of the maximum primary velocity gradient or rate of strain. This statement is equivalent to writing

$$\epsilon = \frac{-\overline{uv_\beta}}{\partial U/\partial \beta} = \frac{-\overline{uv}}{\partial U/\partial y} = \frac{-\overline{uw}}{\partial U/\partial z}, \tag{3}$$

where, if $\partial V/\partial x$ and $\partial W/\partial x$ are small and negligible, ϵ is an eddy viscosity coefficient, isotropic in the y, z or α, β plane. In the slowly-developing or fully-developed boundary region, dominated by secondary currents of the second

kind, it is thus reasonable to expect that the primary shear stress $\overline{uv_{\beta_1}}$ will remain aligned to the mean rate of strain when the flow field is distorted, both by the shape of the boundary and by induced secondary currents.

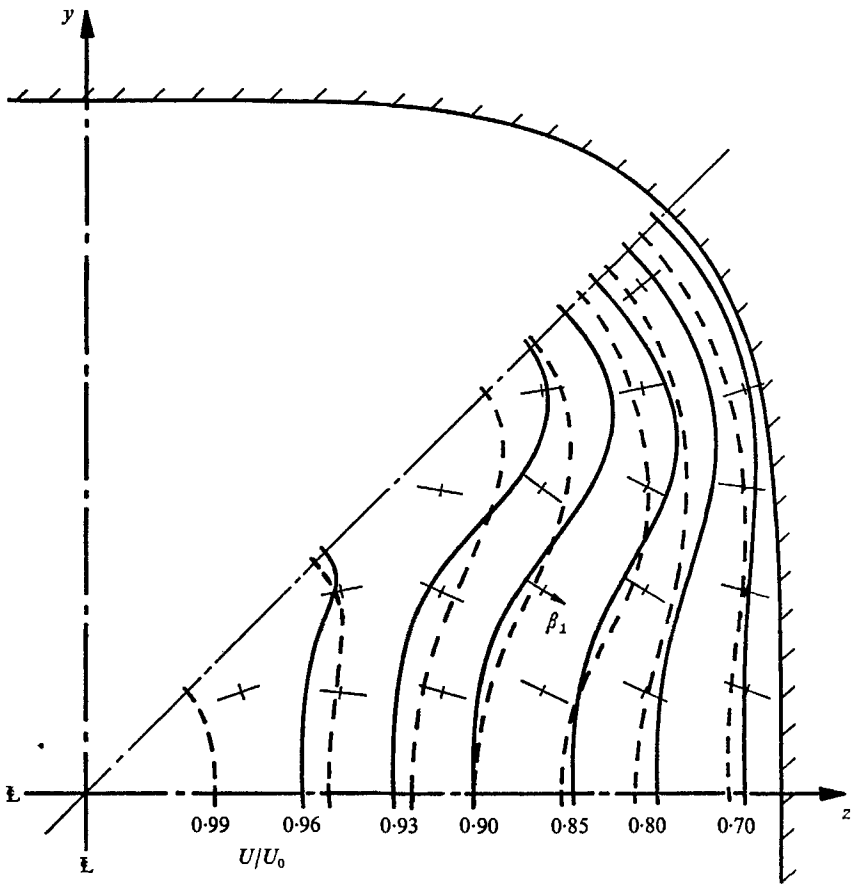

FIGURE 5. Direction of resultant shear stress, $\overline{uv_\beta} = (\overline{uv}^2 + \overline{uw}^2)^{\frac{1}{2}}$, in a superelliptic conduit $Re = 123{,}400$ (after Perkins 1967). ——, hot-wire isovels; – – –, total pressure tube isovels.

An additional feature of the resultant shear stress, defined in the above manner, is its apparent proportionality to the turbulence kinetic energy. In the corner boundary layer the constant of proportionality varies between 0·114 and 0·183 taking its lowest values along the corner bisector plane.

(*b*) *The secondary shear stress,* $\overline{vw}$

Unlike a conventional shear stress, which is strongly correlated with the mean shear, the secondary shear stress $\overline{vw}$ is composed of two parts in the boundary region. The first, $\overline{vw}_1$, is of conventional form, having a magnitude largely determined by the local skewing, and is frequently written in terms of the isotropic eddy viscosity coefficient as

$$\overline{vw}_1 = -\epsilon(\partial W/\partial y + \partial V/\partial z) = \overline{uv}\,\frac{\partial W/\partial y + \partial V/\partial z}{\partial U/\partial y + \partial V/\partial x}. \tag{4}$$

Such a statement automatically assumes an instantaneous adjustment in the shear stress field, both in magnitude and direction, in response to an adjustment in the mean shear.

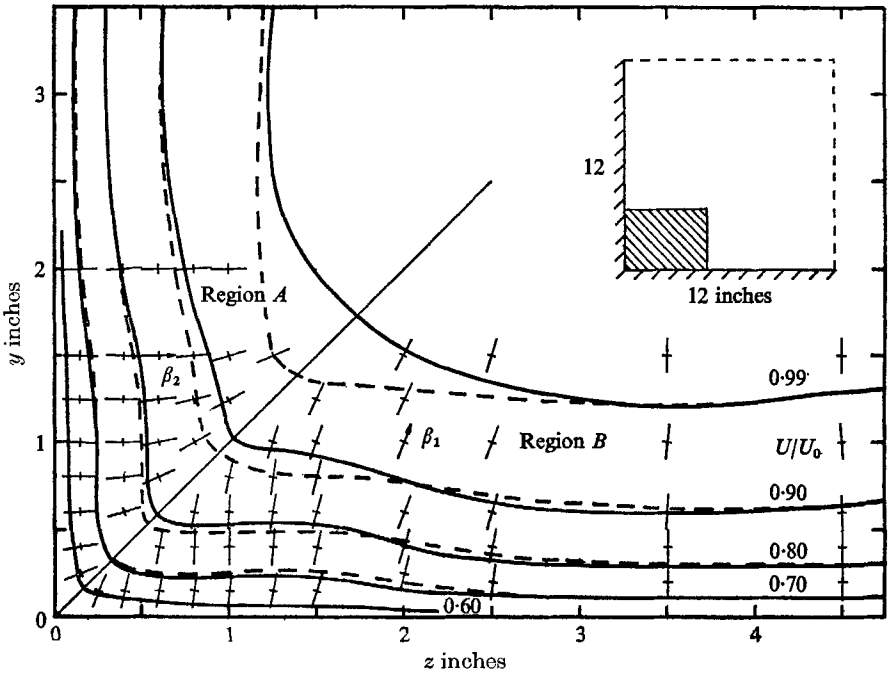

FIGURE 6. The corner boundary layer ($U_0 = 56{\cdot}70$ ft./sec, $\partial p/\partial x \approx 0$). Region A: orientation of planes in which $(\overline{v_\alpha v_\beta})_2 = 0$. Region B: direction of resultant shear stress

$$\overline{uv_\beta} = (\overline{uv}^2 + \overline{uw}^2)^{\frac{1}{2}}.$$

——, total pressure tube isovels; – – –, hot-wire (X-probe) isovels.

The second part, $\overline{vw}_2 = \overline{vw} - \overline{vw}_1$, is peculiar to the boundary region, being induced through the distortion of the direct stress field by the changing shape of the boundary. Its magnitude will depend primarily on the degree of distortion, being zero in the transverse homogeneous flow and comparable with the primary shear stress in a severe boundary region. Consider the force equilibrium of the fluid element shown in figure 7. Neglecting (i) the transverse changes in momentum across the element (which gave rise to $\overline{vw}_1$), and (ii) streamwise gradients in the primary shear stresses, then

$$(\overline{v_\alpha v_\beta})_2 = 0 \quad \text{when} \quad \tan 2\psi = -2\overline{vw}_2/(\overline{v^2} - \overline{w^2}) \tag{5}$$

by elementary principal stress analysis. In figures 4 (region B) and 6 (region A) the calculated orientations of planes in which the second part of the secondary shear stress $\overline{v_\alpha v_\beta}$ vanishes are shown as β_2 planes. In each case the correlation $(\overline{v_\alpha v_\beta})_2$ would appear to be zero in a simple, or natural, orthogonal co-ordinate system having the solid surface as one boundary and the duct centre-line or free-

stream boundary as the other. Hence $\overline{vw}$ is small when the (x, α_2, β_2) co-ordinate system is similar in form to the base Cartesian system, and takes its greatest values where the two systems are most dissimilar. This statement is consistent with the experimental observations and explains why $\overline{vw}$ should take significant

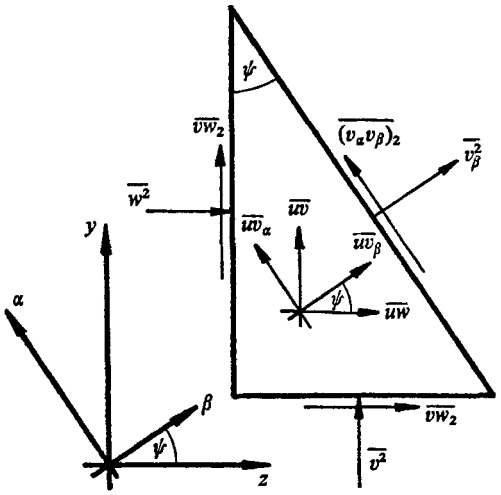

FIGURE 7. A fluid element under stress.

values along the bisector of the right-angled corner or in the elliptic duct where secondary flows are extremely small but the conduit boundaries are non-planar. $\overline{vw}_2$ in the above expression was obtained by subtracting from the measured shear stress the component $\overline{vw}_1$ calculated from equation (4). The observations were found to be unchanged when $\overline{vw}$ replaced $\overline{vw}_2$ in the expression, the angle ψ being relatively insensitive to the value of the numerator in the bisector region where $(\overline{v^2} - \overline{w^2})$ approaches zero.

Gessner's experimental location of planes in which the secondary shear stress vanishes are in complete agreement with the above observations, although a consequence of this analysis suggests that the principal direct stresses are oriented such that the ratio $\overline{v_\alpha^2}/\overline{v_\beta^2}$ takes its maximum value in the (α_2, β_2) co-ordinates, not in the isovel co-ordinates suggested by Gessner.

In the introduction the terms P_2, P_3 and P_4 are collectively referred to as sources of streamwise vorticity of Prandtl's second kind. The above observations would suggest that this statement requires qualification. Having divided $\overline{vw}$ into two parts, a similar division must now arise in P_4, the component P_{4_1} being associated with secondary flows of the first kind, whereas P_{4_2} is analogous to P_3. Further, since $\overline{vw}_1$ is very much dependent on the current form of the streamwise vorticity field, P_{4_1} is unlikely to represent a production term having more the role of a spatial redistribution or diffusion term. Only the component P_{4_2} will represent a source of streamwise vorticity of the second kind. The interchangeability of $\overline{vw}_2$ and $(\overline{v^2} - \overline{w^2})$ by the above expression extends also to the production terms P_{4_2} and P_3, as pointed out by Brundrett & Baines.

(c) *The anisotropic direct stresses*

According to Prandtl's hypothesis, and previous investigations, the most important term in equation (1) is P_3, the production of streamwise vorticity by the anistropy of the transverse direct stresses. A detailed examination of this difference is therefore warranted.

The kinetic energy of the velocity fluctuations in a turbulent boundary layer is, in general, shared unequally between the velocity components in any three mutually perpendicular directions; that is, the turbulence is anisotropic and $(\overline{v^2}-\overline{w^2})$ is non-zero. Curve 4 in figure 11 shows, for example, this difference in Klebanoff's (1954) zero-pressure-gradient boundary layer developing in the x direction over the $y = 0$ surface. Without discussing the complex processes involved in producing, distributing and eventually dissipating this energy it is possible to account for the form of $(\overline{v^2}-\overline{w^2})$ in terms of simple physical arguments. Within the boundary layer the component velocity fluctuations perpendicular to the solid surface, v, are attenuated or constrained by the proximity of the surface, and so remain less than those parallel to the wall, w. The eddy motions are therefore elliptic when viewed in the y, z plane, the axes of the ellipse being aligned to the β_2 co-ordinates, discussed above. Consequently the difference between $\overline{v^2}$ and $\overline{w^2}$ will be most strongly dependent on the distance from the surface. This ceases to be true on approaching the wall, where v and w are rapidly damped by the fluid viscosity, w first rising to a peak following closely the form of u, which is strongly Reynolds-number dependent. Non-dimensionalizing the Reynolds stresses with u_τ, the local wall shear velocity, it should be possible for regions not too close to the wall to write

$$(\overline{v^2}-\overline{w^2})/u_\tau^2 = f(y/l), \tag{6}$$

where l is the characteristic length y at which $\overline{v^2} = \overline{w^2}$, or to a close approximation, δ the thickness of the boundary layer at the point where $U = 0{\cdot}995U_0$, and f is a universal function. The term 'local' refers to the value of u_τ at the position on the wall nearest to the point in question.

Figure 10 shows experimental measurements of $(\overline{v^2}-\overline{w^2})$ collected in the non-uniform boundary layer developing on one wall of the author's duct at points away from the corner region. When plotted in the form (6) (note that the boundary layer is on the $z = 0$ surface so that z replaces y in (6), and f changes sign) the data collapse onto a common curve for different values of u_τ and δ. For the corner boundary layer, where each side of the corner bisector plane is considered separately, the data are plotted according to the above model in figure 9, l having the distribution shown inset. Similarly in the square duct, figure 8, the data of Gessner reduce to a single curve for the chosen distribution $l(z)$. The results for the four experiments discussed above are summarized as figure 11 for comparison. All the curves are in agreement as to the basic form of $(\overline{v^2}-\overline{w^2})$ but disagree on the absolute magnitude. This discrepancy is attributable to four main sources: (i) A genuine non-universality. (ii) Experimental errors in measuring $(\overline{v^2}-\overline{w^2})$. The maximum scatter expected in the results for each 1 %

reading error in v and w is shown superimposed on figure 11 and clearly could account for much of the discrepancy. (iii) Variations in interpretation of inclined hot-wire signals in the various experiments. Errors in estimating the function

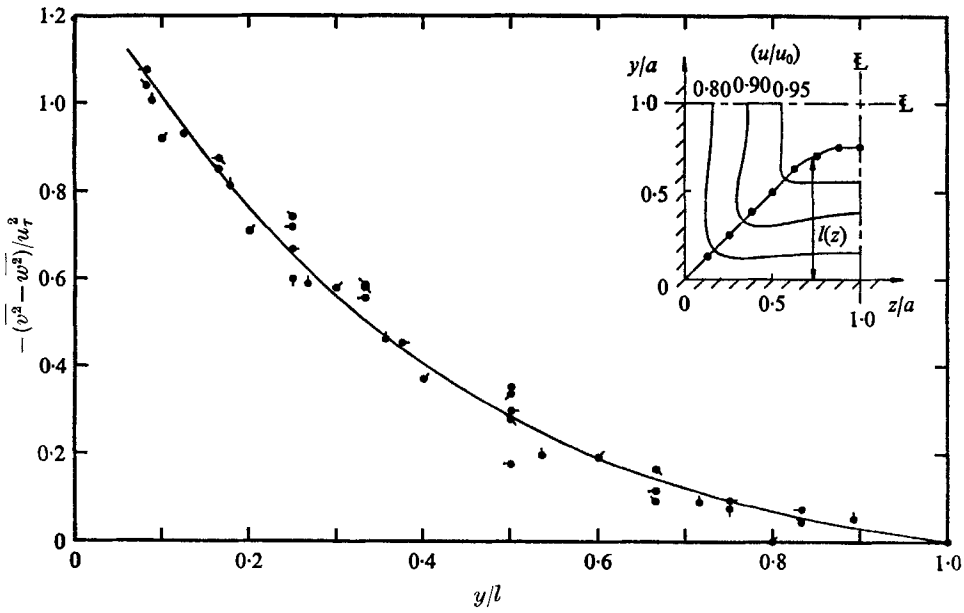

FIGURE 8. $(\overline{v^2}-\overline{w^2})$ in a square duct, Re = 150,000 (after Gessner 1964). Values of z/a and l/a: ●, 1·00, 0·750; ●, 0·875, 0·750; ●, 0·750, 0·750; ●, 0·625, 0·625; ●, 0·500, 0·500; ●, 0·375, 0·375; ●, 0·250, 0·250; ●, 0·125, 0·125.

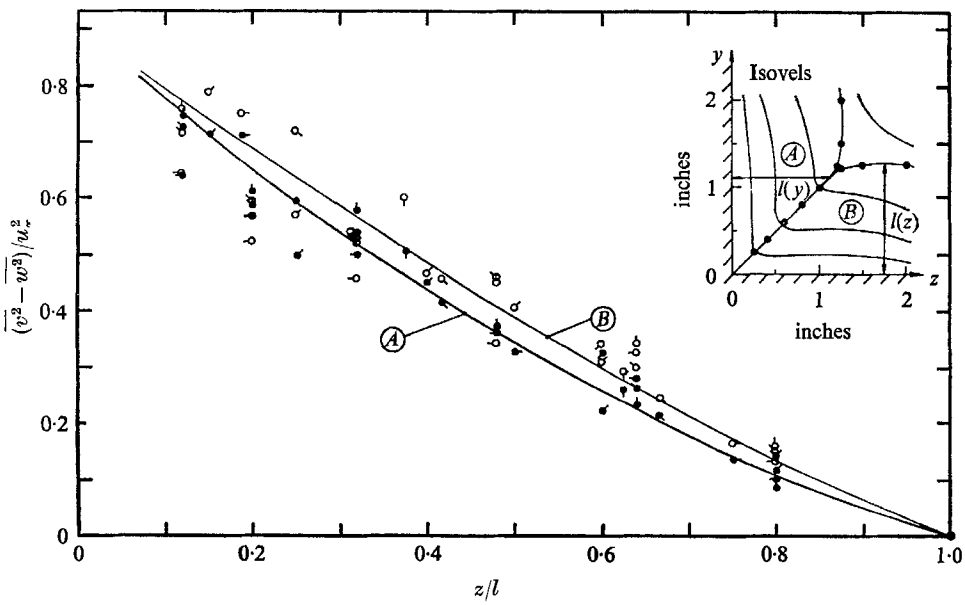

FIGURE 9. $(\overline{v^2}-\overline{w^2})$ in the corner layer. Open symbols refer to region B. Values of y in inches: ●, 2·00; ●, 1·50; ●, 1·25; ●, 1·00; ●, 0·80; ●, 0·60; ●, 0·40; ●, 0·25.

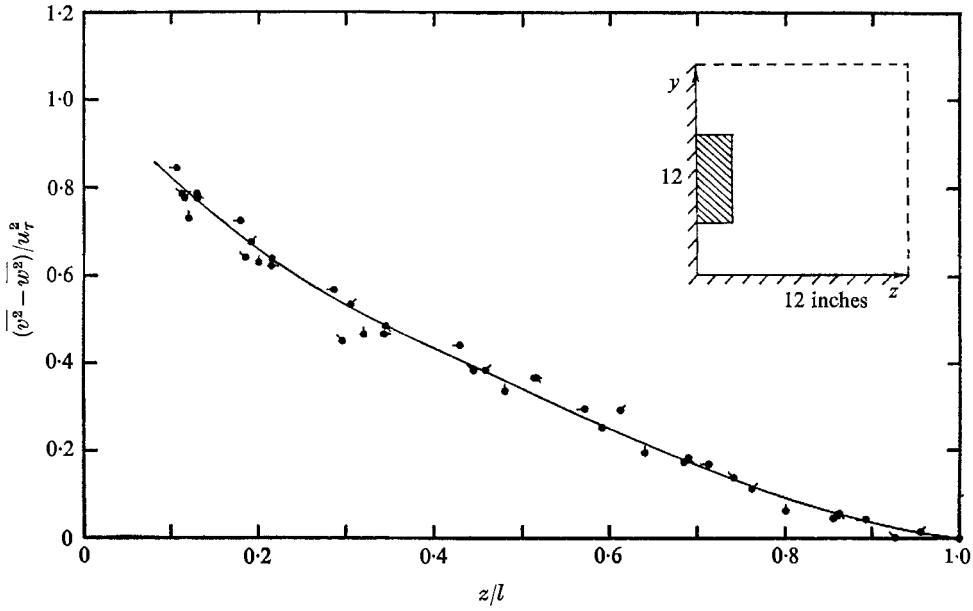

FIGURE 10. $\overline{(v^2-w^2)}$ in a non-uniform nominally two-dimensional boundary layer.

Symbol	●	◔	◑	◕	●	●
y (inches)	8·0	7·0	6·0	5·0	4·0	3·0
δ (inches)	1·40	1·35	1·25	1·31	1·17	1·16
u_τ/u_0	0·0336	0·0340	0·0346	0·0342	0·0347	0·0349

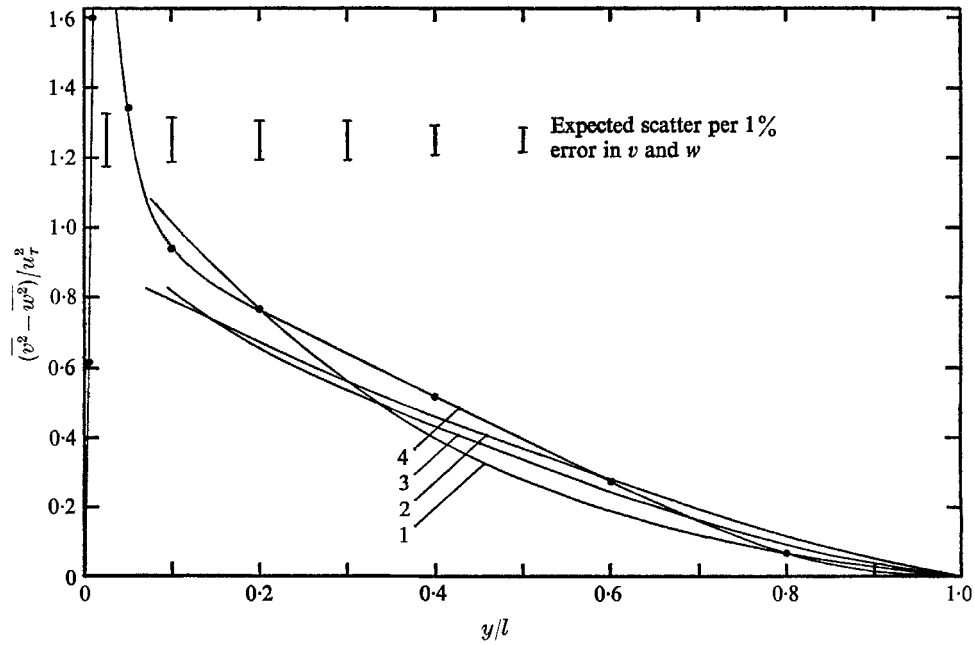

FIGURE 11. Summary of $\overline{(v^2-w^2)}$ data. Curve: 1, square duct flow (figure 8); 2, corner layer (figure 9); 3, non-uniform boundary layer (figure 10); 4, Klebanoff zero-pressure-gradient boundary layer.

$g(\theta)$ (appendix) in the X-probe response equation will clearly be reflected in the $\overline{v^2}$ and $\overline{w^2}$ measurements. Gessner has assumed that $n = m = \frac{1}{2}$, whereas Klebanoff has used X-probes of increased transverse sensitivity (60 degrees included angle) for which the yaw response is, in general, ill defined. (iv) Experimental errors in estimating u_τ, one of the most difficult boundary-layer quantities to measure.

Bearing in mind the above sources of error, it is reasonable for the present to write the anisotropic stress $(\overline{v^2}-\overline{w^2})/u_\tau^2$ as a universal function of y/l (or z/l) for $y/l > 0{\cdot}1$, where l describes a curve along which $\overline{v^2} = \overline{w^2}$.

The natural extension of this model in a diffusing boundary-layer flow is described in Perkins (1970).

3. The terms of the streamwise vorticity equation

Each term in equation (1) can be deduced from the secondary flow or Reynolds stress measurements by taking spatial derivatives of at least second order, a highly inaccurate process when applied to the $\overline{vw}$ and $(\overline{v^2}-\overline{w^2})$ data. However, by averaging the data gathered on each side of the bisector plane in the corner boundary layer at two measurement stations along the duct 12 inches apart, it was possible to arrive at the distributions shown as contours in figure 12. Such a procedure necessarily assumes that each of the four sets of data implied above represents an independent assessment of the same event. Of the terms involving a streamwise derivative P_1, P_2 and $\xi\,\partial U/\partial x$ were found to be negligible over the test area, $2 \geqslant y$ (and z) $\geqslant 0{\cdot}15$ inches, whilst $U\,\partial\xi/\partial x$, for which only one estimate was possible, varied erratically having the qualitative form indicated. These calculations suggest that the terms P_3 and P_4 are of equal order contrary to previous calculations by the author and by Brundrett & Baines in fully-developed square duct flow, where P_4 tended to be negligible. The resulting form of equation (1) in the slowly-developing corner boundary layer is thus

$$U_s\,\partial\xi/\partial s = \nu(\partial^2\xi/\partial y^2 + \partial^2\xi/\partial z^2) + P_3 + P_4, \tag{7}$$

where the viscous diffusion, although negligible over the above-mentioned test area, is retained to balance the near-wall production of streamwise vorticity where U_s is small and vanishing. The importance of P_3 in generating the observed secondary currents is here confirmed and in addition the significance of the transport term P_4 has been demonstrated. It was found impossible to separately compute P_{4_1} and P_{4_2} with any degree of confidence, although the two components were thought to be of approximately equal order over the test area.

4. Application of the simplified streamwise vorticity equation

In the developing boundary-layer situation, (7) must be solved in conjunction with the streamwise momentum equation and the continuity condition, whereas in fully-developed duct flows the former is readily soluble, in isolation, for $\xi(y, z)$ given the distribution of the Reynolds stresses $\overline{vw}$ and $(\overline{v^2}-\overline{w^2})$, or equivalently P_3 and P_4. Unfortunately experimental data in near-wall regions are at present

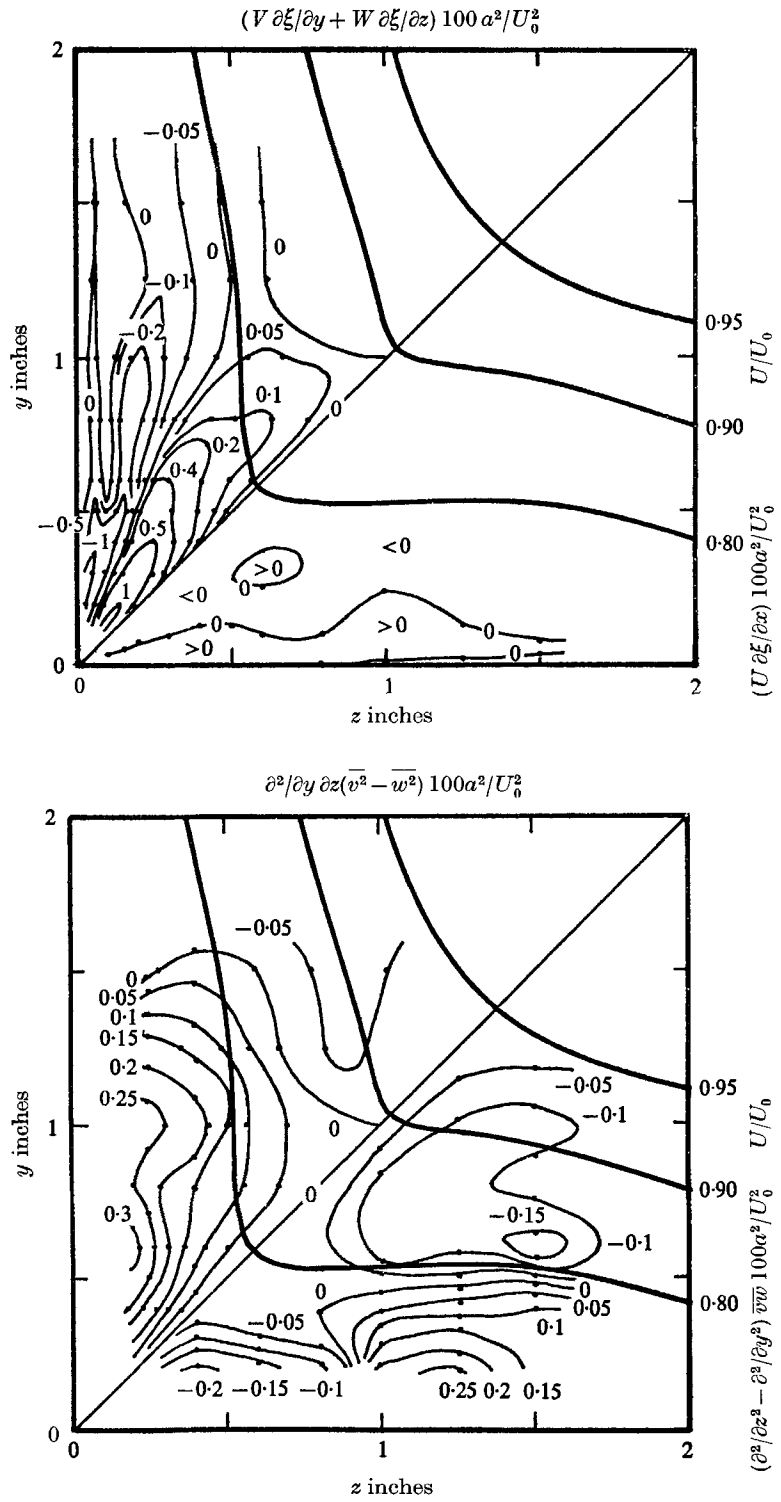

FIGURE 12. Terms in the streamwise vorticity equation, corner boundary layer, $a = 1{\cdot}3$ inches, $U_0 = 56{\cdot}5$ ft./sec.

lacking, precluding such a solution. Nevertheless, it is possible to employ this simplified equation qualitatively in deducing only the *direction* of the secondary currents arising in response to a production field determined by the flow geometry.

Integrating (7) along the local mean streamline, which will have an approximately helical form in the spiral secondary currents, then

$$\xi - \xi_0 = \int_{s_0}^{s} (1/U_s)(P_3 + P_4)\, ds, \tag{8}$$

neglecting the viscous diffusion term away from the solid surface. This statement suggests that the streamwise vorticity should tend to adopt the sign of the quantity $(P_3 + P_4)$ in the outer flow, if the latter is predominantly of one sign. This is demonstrably true of the corner boundary layer where the vorticity field ξ in figure 3 takes the sign of $(P_3 + P_4)$, or of P_3 if P_4 is dropped to simplify the argument. It should be noted that all the terms in (1), and in addition ξ and $(\overline{v^2} - \overline{w^2})$, are antisymmetric about the corner bisector plane.

If it is assumed that this empirical observation will apply equally to any boundary-region-type flow, then it is possible to determine the *direction* of the outer region secondary currents (given by the local sign of the streamwise vorticity), simply by knowing the *sign* of P_3. From the model proposed earlier for $(\overline{v^2} - \overline{w^2})$, the local production is given by

$$P_3 = -\frac{u_\tau^2}{l}\left(\frac{1}{l}\frac{\partial l}{\partial z}\left(\frac{y}{l}f'' - f'\right) - \frac{2}{u_\tau}\frac{\partial u_\tau}{\partial z}f'\right), \tag{9}$$

where the dash denotes differentiation with respect to (y/l). Since only the sign of this term is required here, the exact behaviour of f is not terribly important, the consequences of the model being adequately demonstrated by the approximation

$$f(y/l) = -(1 - y/l),$$

which gives for the production

$$P_3 = \frac{u_\tau^2}{l}\left(\frac{2}{u_\tau}\frac{\partial u_\tau}{\partial z} - \frac{1}{l}\frac{\partial l}{\partial z}\right). \tag{10}$$

Mean streamwise vorticity is therefore produced by the anisotropy of the turbulence when a transverse gradient arises in u_τ and/or l, the chosen parameters. By considering the distributions of these quantities in various examples, the direction of the induced secondary currents will be deduced.

(*a*) *The nominally two-dimensional boundary layer*

Still concentrating on slowly-developing flows, the type of boundary layer implied here has the form illustrated in figure 13, containing a transverse periodic deformation in u_τ and/or δ. Application of equation (10), with $l = \delta$ the local thickness of the layer, suggests the following properties: (i) In planes such as B–B', which locally constitute planes of flow symmetry, $\partial u_\tau/\partial z$ and $\partial\delta/\partial z$ are zero so that P_3, and consequently ξ by the arguments presented above, are also zero. (ii) In planes of type A–A', u_τ is increasing and δ decreasing, giving a production greater than zero and hence a clockwise secondary current. (iii) For

C–C', which is a mirror image of A–A', the reverse is true, suggesting a family of secondary flow cells distributed along the surface each of opposite rotation to its immediate neighbours, as illustrated.

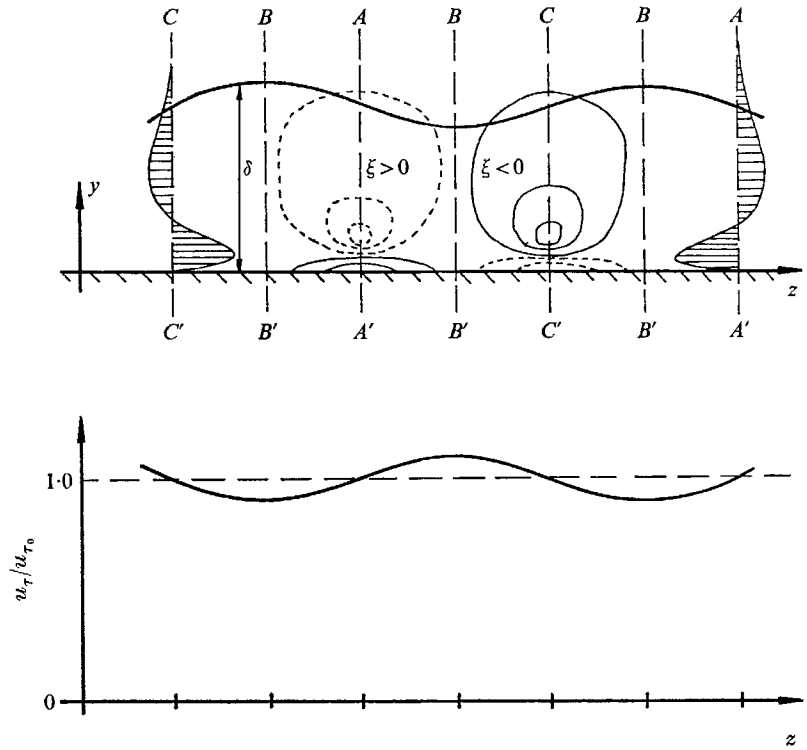

FIGURE 13. Model for non-uniform boundary layer. ——, – – –, lines of constant ξ.

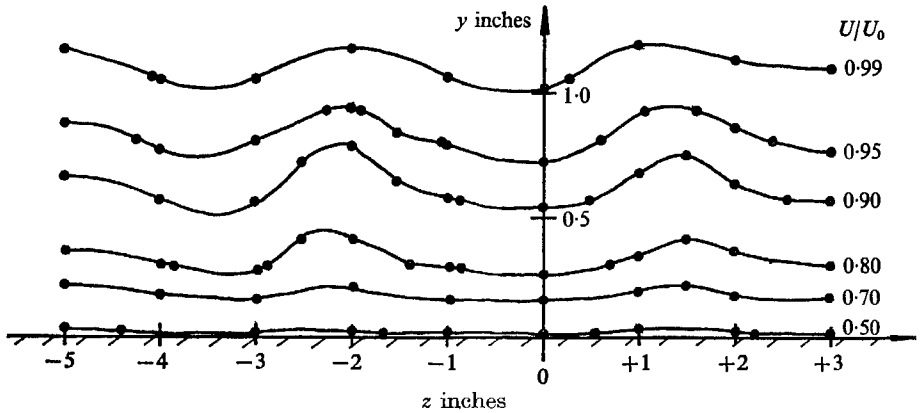

FIGURE 14. The non-uniform nominally two-dimensional boundary layer (after de Bray 1967) (—●—●—, interpolated from de Bray's data).

Secondary currents of the second kind are therefore present in this layer and directed in such a way as to maintain or amplify the existing flow deformations. This deduction is consistent with the 'peak–valley' formation commonly encountered in nominally two-dimensional boundary-layer flows and originally

demonstrated by Klebanoff & Tidstrom (1959). The origin of the non-uniformities, which are not themselves spontaneously produced by the turbulence, remains a subject for debate. By systematically testing various combinations of screens, honeycombs and transition devices, de Bray (1967) succeeded in confirming the findings of Bradshaw (1965) that the transverse irregularities originate behind wind-tunnel screens, the degree of non-uniformity being simply a function of the screen blockage. Figure 14 shows the cross-section through a boundary layer measured by de Bray using a very unfavourable screen configuration. The variation in u_τ amounts to $\pm 8\,\%$ and in δ, $\pm 12\,\%$. The data presented in figure 10 were also collected in a non-uniform boundary layer having only a $\pm 2\,\%$ variation in u_τ (the experimental scatter probably exceeds $\pm 2\,\%$) but a $\pm 10\,\%$ variation in δ.

(*b*) *The salient edge flow*

The experimental results of Elder (1960) for flow along the streamwise edge of a finite flat plate are presented as figure 15. Elder established the existence of weak secondary currents in regions C and F and suggested that they were of the type already familiar in fully-developed duct flows. Since the anisotropy model proposed earlier is valid only for wall turbulence it is unlikely to apply beyond the edge of the surface where v and w have approximately the same magnitude.

In region B, however, where $l = \delta$, u_τ is increasing in z while δ decreases, so that P_3 and ξ are positive. Clockwise secondary currents in this region are consistent with the negative vorticity observed by Elder in the neighbouring region. The reverse will be true of region E, which is a mirror image of B.

An alternative model for the stress difference $(\overline{v^2} - \overline{w^2})$ must be devised for regions C and F, but since $\overline{v^2} \approx \overline{w^2}$ it is unlikely to explain the vorticity production there. Although the author was unable to locate stress tensor measurements in the vicinity of an edge, it is to be expected, by the arguments of § 2(*b*), that $\overline{vw}$ and consequently P_4 will dominate in this region. Since the two stresses $\overline{vw}_2$ and $(\overline{v^2} - \overline{w^2})$ can be interchanged through a co-ordinate rotation it should be possible to construct a system of co-ordinates (x, α, β) in which $(\overline{v_\alpha v_\beta})_2 = 0$ and $(\overline{v_\alpha^2} - \overline{v_\beta^2})$ has the form already described. Such a co-ordinate system would intuitively be of polar form centred on the edge. Assuming the edge has a finite radius of curvature R, then, in terms of the cylindrical polar co-ordinates (x, r, ϕ) shown in figure 15, let

$$(\overline{v_r v_\phi})_2 \approx 0 \quad \text{and} \quad (\overline{v_r^2} - \overline{v_\phi^2})/u_\tau^2 = f\left(\frac{r-R}{l}\right),$$

where $l = \delta$, the radial distance from the edge to the free stream. The vorticity production becomes

$$P_3 = \frac{1}{r}\left(\frac{1}{r}\frac{\partial}{\partial \phi} - \frac{\partial^2}{\partial r\, \partial \phi}\right)(\overline{v_r^2} - \overline{v_\phi^2}),$$

which, using again the simple function

$$f\left(\frac{r-R}{l}\right) = -\left(1 - \frac{r-R}{l}\right),$$

reduces to $$P_3 = -\frac{u_\tau^2}{r^2}\left[\frac{2}{u_\tau}\frac{\partial u_\tau}{\partial \phi}\left(1-\frac{2r-R}{\delta}\right)+\frac{1}{\delta}\left(\frac{2r-R}{\delta}\right)\frac{\partial \delta}{\partial \phi}\right].$$

(i) Along the plane of symmetry $\phi = \frac{1}{2}\pi$, both $\partial u_\tau/\partial\phi$ and $\partial\delta/\partial\phi$ are zero, secondary flows being absent. (ii) For $0 < \phi < \frac{1}{2}\pi$, δ is increasing in ϕ, the boundary-layer thickness doubling over the interval, whereas u_τ remains

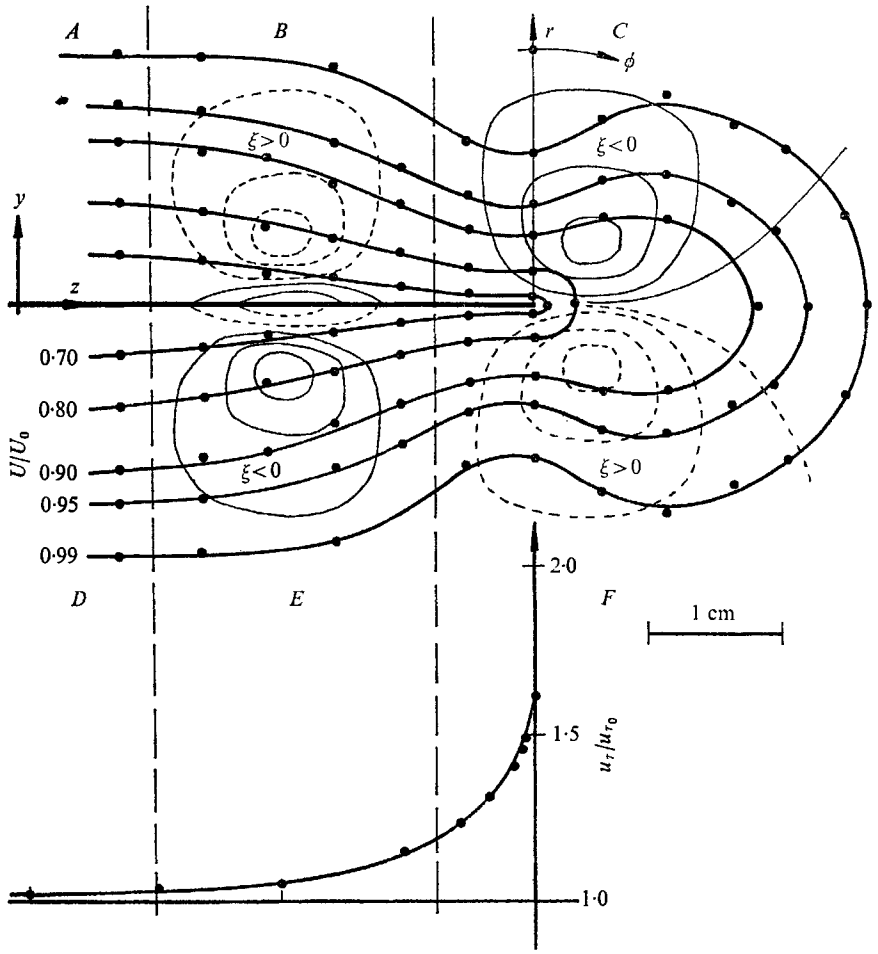

FIGURE 15. The edge flow (after Elder 1960). ——, – – –, lines of constant ξ.

approximately constant. Hence, negative vorticity is induced in this region. (iii) For $\frac{1}{2}\pi < \phi < \pi$ the reverse is true and the vorticity is positive. The secondary currents suggested by the revised anisotropy model are entirely consistent with Elder's observations. In regions A and D it is unlikely, recalling the previous example, that secondary currents will be entirely absent.

(c) *The corner boundary layer*

The similarity between the slowly-developing corner layer and fully-developed square duct flow, both in the strength, scale and direction of the secondary motions and in the details of the Reynolds stress tensor, has been established, so

that qualitative arguments presented here for the former will apply equally to the latter. By retaining the Cartesian co-ordinate system in which $(\overline{v^2}-\overline{w^2})$ has been successfully modelled and an expression for P_3 devised, additional constraints must be imposed in satisfying the symmetry requirements in the bisecting plane. In this plane, $y = z = l$, the production P_3 must be zero, so that

$$f''(1) = f'(1)\left(\frac{2z}{u_\tau}\frac{\partial u_\tau}{\partial z} - 1\right)$$

from equation (9), or, since f is a universal function, u_τ varies as a power of z. Such a variation is supported by the author's data, although Preston tube estimates of u_τ near to the corner line must be viewed cautiously as the region correlated by the 'inner law' diminishes and probe blockage effects become largely indeterminate.

Continuing the arguments used in the previous two examples then,

$$P_3 = \left(\frac{u_\tau}{z}\right)^2\left[\frac{2z}{u_\tau}\frac{\partial u_\tau}{\partial z} - 1\right]$$

for the region where $l = z$. Since $\partial u_\tau/\partial z$ is less than $u_\tau/2z$, the power law index being less than $\frac{1}{2}$, then P_3 and consequently ξ will be negative. On the opposite side of the bisector plane the vorticity will be of reversed sign.

Further from the corner line the arguments and the conclusions are as before, suggesting that an entirely homogeneous asymptote to the corner layer is unlikely. It is to be expected that the terms P_1 and P_{4_1}, associated with the mutual skewing of the two layers, will dominate in this region, but unfortunately it has not been possible to confirm this from the present experimental data.

The author is indebted to Professor J. H. Horlock who has supervised the research described here and assisted in the preparation of this paper.

Appendix. Corner boundary-layer experiments

A square-sectioned duct 12 inches wide and 66 inches in length was attached to the $14\frac{1}{2}$ inch square exit of a blower wind tunnel, in such a way that two sides of the duct formed a continuation of the wind tunnel walls. The remaining two sides, having sharp leading edges, were machined to form an accurate right-angled corner, the test corner. The former pair of sides were constructed from perforated sheet steel, the perforations remaining blanked off on the inside for the experiments described here, and the latter pair were of Perspex. Construction of the wind tunnel and the duct was such that geometric symmetry about the bisector of the test corner was maintained to a high accuracy. The boundary layers developing from the leading edge of the solid surfaces were tripped by a wire 0·1 inches in diameter placed 2·25 inches from the leading edge. A slightly favourable streamwise pressure gradient persisted throughout the length of the duct.

Reynolds stresses were measured using an 'X' array hot-wire probe rotated in the flow relative to the Cartesian co-ordinate system in which the stresses were required. The plane of the X-probe is aligned in turn to the x, y and x, z planes and to two intermediate planes at 45 degrees to the y direction. The six stresses

are deduced from nine r.m.s. voltages, the readings taken in each orientation being chosen so that each stress depends on a maximum of two measured quantities. In the response equation used by the author the heat loss from the constant-temperature wire is written in terms of three almost separable functions of ambient temperature, velocity and yaw angle:

$$E^2 - E_0^2 = KU^n \sin^m \theta,$$

where E is the instantaneous bridge voltage, E_0 the bridge voltage at zero flow, θ the instantaneous inclination of the wire to the velocity vector, and $K(U)$, $n(U)$, and $m(U, \theta)$ are constants for a given velocity, ambient temperature, overheat ratio, and yaw angle. The ratio m/n is thought to be only weakly dependent on U, and strongly dependent on the geometry of a given wire. Hence, the fluctuating bridge voltages for the two wires a and b of the X-probe are

$$e_a = \gamma_a(u + g_a(\theta)v) \quad \text{and} \quad e_b = \gamma_b(u + g_b(\theta)v), \quad \text{in the } x, y \text{ plane},$$

where γ is a function of E, E_0, K, U and n, and $g = (m/n)\cot\bar{\theta}$, $\bar{\theta}$ being the inclination of the wire to the time-averaged velocity vector. The exponent n must be determined from a $(E^2 - E_0^2)$ *versus* U calibration (preferably with $\bar{\theta}$ set at 90 degrees), and $m/n(\theta)$ from a yaw calibration. For the latter, the Reynolds shear stress was measured in a pipe, $3\frac{1}{2}$ inches in diameter and approximately 100 diameters in length, and compared to that predicted by the axial pressure drop.

Mean secondary currents were deduced from hot-wire yaw measurements in the x, y plane only. Flow symmetry about the corner bisector plane was assumed in calculating Q, the resultant secondary flow vectors illustrated.

REFERENCES

Bradshaw, P. 1965 *J. Fluid Mech.* **22**, 679–687.

Brundrett, E. 1963 Ph.D. Thesis, University of Toronto, TP 6302.

Brundrett, E. & Baines, W. D. 1964 *J. Fluid Mech.* **19**, 375–392.

de Bray, B. G. 1967 *Aero. Res. Counc. R & M* 3578.

Einstein, H. A. & Li, H. 1958 *Amer. Geophysical Union*, **39**, 1085–1088.

Elder, J. W. 1960 *J. Fluid Mech.* **5**, 133–153.

Gessner, F. B. 1964*a* Ph.D. Thesis, Purdue University.

Gessner, F. B. 1964*b* *ASME paper* 64-WA/FE-34.

Gessner, F. B. & Jones, J. B. 1961 *J. Basic Engng ASME*, **83**, 657.

Gessner, F. B. & Jones, J. B. 1965 *J. Fluid Mech.* **23**, 689–713.

Hawthorne, W. R. 1951 *Proc. Roy. Soc.* A **206**, 374.

Hinze, J. O. 1967 *Phys. Fluids*, Suppl. **10**, S 122–S 125.

Klebanoff, P. S. & Tidstrom, K. D. 1959 *NASA TN* D-195.

Klebanoff, P. S. 1954 *NACA TN* 3178 (or *NACA Rep.* no. 1247, 1955).

Perkins, H. J. 1967 M.A.Sc. Thesis, University of Waterloo.

Perkins, H. J. 1969 *Cambridge University Internal Rep.* CUED/A-Turbo/T.R.8 (or *Aero. Res. Counc.* 31 748-F.M. 4118-Turbo. 95).

Perkins, H. J. 1970 Ph.D. Thesis, Cambridge University.

Prandtl, L. 1952 *Essentials of Fluid Dynamics.* London: Blackie.

Squire, H. B. & Winter, K. G. 1951 *J. Aero Sci.* **18**, 271.

Taylor, E. S. 1959 *J. Basic Engng ASME*, **81**, 297–304.